

# Metamorphic Evolution of the Tønsvika Eclogite, Tromsø Nappe—Evidence for a New UHPM Province in the Scandinavian Caledonides

E. J. KROGH RAVNA<sup>1</sup> AND M. R. M. ROUX

*Department of Geology, University of Tromsø, N-9037 Tromsø, Norway*

## Abstract

Eclogites within the Tromsø Nappe of the Uppermost Allochthon in the Scandinavian Caledonides record a complex P-T history, involving a prograde subduction-related stage. Information on the early prograde stage of the metamorphic evolution is provided by a relict amphibolite-facies inclusion suite within garnet. The inclusion assemblage comprises hornblende, oligoclase, albite, paragonite, biotite, and quartz. Included hornblende is chemically distinct from the secondary hornblende appearing in the matrix. Thermobarometric estimates on included hornblende and oligoclase yield pressures of ca. 1.3 GPa at 600–700°C. Maximum pressure conditions recorded are 3.36 GPa at 735°C, based on coexisting garnet, omphacite, and phengite, well within the coesite stability field. Post-eclogite decompression resulted in omphacite decomposition to three successive diopside + plagioclase symplectite stages: S1, S2, and S3. The width of the lamellar spacing (L) and the composition of the clinopyroxene vary as follows:  $L_{S1} > L_{S3} > L_{S2}$  and  $X_{Jd}^{S1} > X_{Jd}^{S2} > X_{Jd}^{S3}$ , indicating that the three symplectites were formed at different P-T conditions. Thermobarometric estimates give 840°C at 1.41 GPa for S1, 700°C at 1.12 GPa for S2, and 740°C at 0.98 GPa for S3. Recrystallization under amphibolite-facies conditions occurred at 650–700°C, 0.9–1.0 GPa. The geothermobarometric results, together with previously published age dating of the rocks, indicates that initial uplift rates were very high, estimated at 3.6 cm/yr.

## Introduction

ECLOGITES AND RELATED rocks within high-pressure (HP) and ultrahigh-pressure (UHP) terranes have been thoroughly studied during the last three decades, and the knowledge of worldwide distribution of such terranes is steadily increasing. The distinction between high-pressure (HP) and ultrahigh-pressure (UHP) metamorphism can be summarized in the definition of UHP metamorphism as “a type of metamorphism that occurs at very high lithostatic pressures within the eclogite facies but above the stability field of quartz” (Carswell and Compagnoni, 2003, p. 3). UHP metamorphic terranes are mainly results of continental collisions. Carswell and Compagnoni (2003) listed 22 UHPM terranes worldwide, of which four have a less certain status.

The positive recognition of UHP metamorphism relies on the identification of mineral indicators such as coesite or diamond. The preservation of coesite in such terranes is, however, very limited

and indirect petrographic and/or petrologic evidence is needed to support a UHP origin. Inclusions of polycrystalline quartz with associated radial expansion fractures in the host mineral have been taken as firm evidence of the former presence of coesite. Another indirect method is the use of suitable geothermobarometers to estimate maximum pressure conditions for the metamorphism (e.g., Gilotti and Ravna, 2002; Ravna and Terry, 2004).

## Geological Setting

The Tromsø Nappe (earlier Tromsø Nappe Complex; e.g. Krogh et al., 1990), makes up the uppermost part of the Uppermost Allochthon of the Scandinavian Caledonides (Fig. 1). The Tromsø Nappe consists of a sequence of polymetamorphic high-grade metasediments (garnet mica schist, marble, calc-silicate rocks) with frequent bodies of mafic (eclogite and garnet amphibolite) and ultramafic rocks (Krogh et al., 1990; Ravna et al., 2006). Krogh et al. (1990) presented data on eclogites and associated gneisses from this area, indicating

<sup>1</sup>Corresponding author; email: Erling.Ravna@ig.uit.no

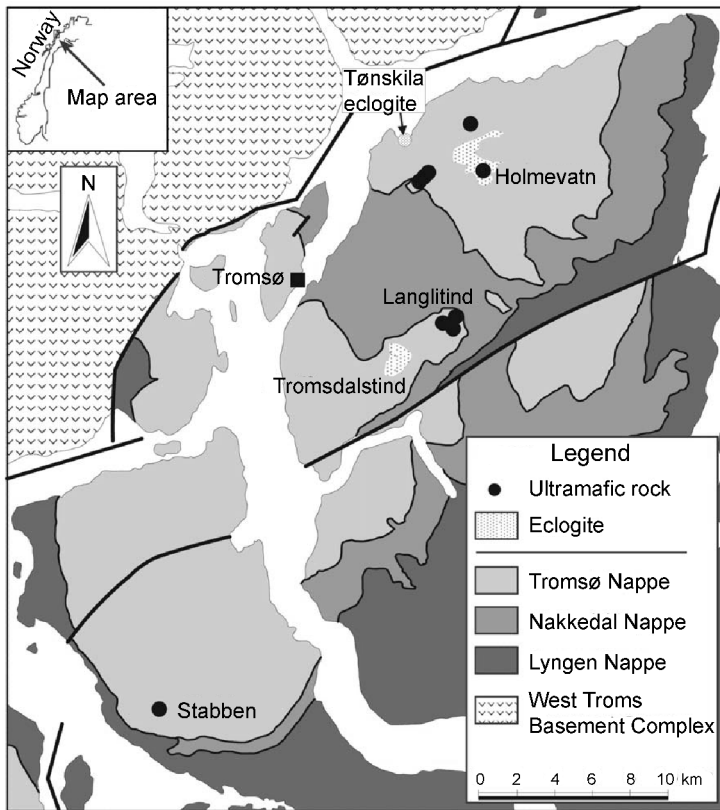


FIG. 1. Tectonostratigraphic map of the Tromsø region, modified after Ravna et al. (2006).

minimum pressures of 1.7–1.8 GPa at 700–750°C, with a later overprint at ~0.8–1.0 GPa/600–650°C. Partial melting of eclogite within the Tromsø Nappe is common (Krogh et al., 1990), and recent work by Stevenson (2005, and pers. com.) confirms two episodes of partial melting. An early episode producing peritectic garnet + melt at 2.0–2.2 GPa, 762–844°C, and a younger one producing peritectic hornblende + melt (garnet being a restite phase) occurred at 1.0–1.3 GPa, 743–950°C (Stevenson, 2005). Ravna et al. (2006) described a prograde subduction-related metamorphic evolution of garnet ultramafics from spinel- to garnet-bearing assemblages, and the subsequent uplift. Cr-bearing spinel and garnet apparently coexisted during subduction over a pressure range from 1.39 to 2.38 GPa at temperatures of 675–740°C. The post maximum-P uplift path includes two temperature maxima—one at ~750–800°C, 1.8 GPa and the second at > 750°C, 1.0 GPa.

Corfu et al. (2003) presented U-Pb zircon and titanite ages for the eclogitic rocks of the Tromsø Nappe. Primary magmatic zircons from a trondhjemitic layer within the large Tromsdalstind eclogite gave an age of 493 +5/-2 Ma, interpreted as the intrusion age of the protolith. Zircons from the Tønsvika eclogite (Figs. 1 and 2), which is studied herein, defined an age of 452.1 ± 1.7 Ma. Slightly younger ages of 451–450 Ma were provided by high-Al titanites from an eclogite and a calc-silicate rock. A low-Al titanite from a post-eclogite hornblende-bearing leucosome gave an age of 450.3 ± 0.9. Rutile fragments from the Tønsvika eclogite gave an age of 428.4 ± 0.8 Ma, interpreted to reflect a resetting during uplift and cooling. These results show that the HP/UHP event and subsequent uplift with partial melting of the eclogite happened within only a few million years (Corfu et al., 2003). A K-Ar age of late hornblende in a retrogressed eclogite gave 437 ± 16 Ma (Krogh et al., 1990). Hornblende

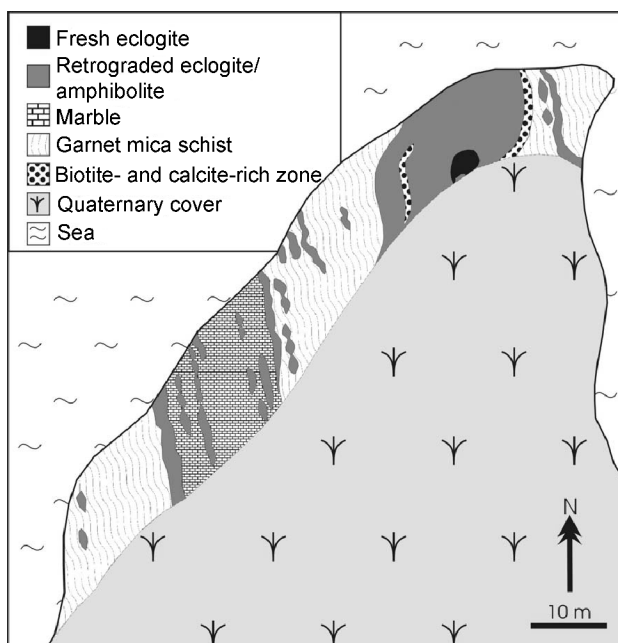


FIG. 2. Detailed map of the Tønsvika eclogite.

$^{40}\text{Ar}/^{39}\text{Ar}$  isotope correlation ages are reported within  $419.4 \pm 2.1$  and  $481 \pm 1.8$  Ma (Dallmeyer and Andresen, 1992) from various parts of the Tromsø Nappe.

The Tromsø Nappe is underlain by the Skattøra migmatite complex (Selbekk et al., 2000), and tectonically separated from it by a major thrust fault (Fig. 1). The Skattøra migmatite complex makes up the upper part of the Nakkedal Nappe Complex and comprises an original Si-undersaturated (nepheline normative) layered mafic complex with layers of anorthositic to ultramafic composition, with gabbroic compositions as the dominant rock type. The rocks have been subject to a high degree of partial melting at high temperatures ( $\sim 900^\circ\text{C}$ ) and high  $\text{H}_2\text{O}$  content, producing a network of anorthositic dikes (Selbekk et al., 2000).

This paper presents petrological evidence for UHP metamorphism of a small eclogite body within the Tromsø Nappe, northern Norway. The eclogite body is located on the 1:50,000 topographic map sheet Tromsø 1534 III, at Tønsvika on the mainland  $\sim 30$  km northeast of the city of Tromsø (Fig. 1). It crops out for about 100 m along the seashore, and the rocks are excellently exposed (Fig. 2).

### Analytical Procedures

Selected mineral compositions are given in Tables 1–6. The samples were analyzed with a JEOL 840 SEM with an EDAX analyzer, using the EDAX SEM-Quant standardless method with optimized SEC factors based on analyses of a set of various mineral standards. Operating conditions were 20 kV accelerating voltage and a beam current of 3 nA. Anhydrous minerals (garnet, spinel, pyroxene, and olivine) are normalized to 100 wt% total, amphiboles to a total of 98 wt%, and mica to 96 wt%.

### Lithology

The studied outcrop (Fig. 1) consists of marble, garnet mica schist/gneiss, and mafic rocks (eclogite and garnet amphibolite). The mafic rocks occur as lenses and boudinaged layers ranging from a few cm up to  $\sim 15$  m in thickness within marble and garnet mica schist (Figs. 2 and 3). The largest lens shows a distinct zoning comprising a massive isotropic core of an essentially bimineralic eclogite with shiny cleavage planes of pristine omphacite, and a foliated flaser-textured marginal zone of partially retrograded eclogite. Spectacular coarse-grained zones

TABLE 1. Data on Diopside-Plagioclase Symplectites, Sample T-54A30

| Zone | Type     | Size         | Average spacing (L) close to the reaction front | X <sub>Na</sub> Cpx | X <sub>Ab</sub> Plag |
|------|----------|--------------|-------------------------------------------------|---------------------|----------------------|
| S1   | Lamellar | Coarse       | 12 μm                                           | 0.23                | 0.15                 |
| S2   | Lamellar | Fine         | 5.5 μm                                          | 0.17                | 0.18                 |
| S3   | Lamellar | Intermediate | 7 μm                                            | 0.15                | 0.14                 |

TABLE 2. Selected Garnet Analyses<sup>1</sup>

| Sample:                        | T-54A3                  |        | T-65   |        | T-68-1 |        | T-68-2          |        | T-41           |        |
|--------------------------------|-------------------------|--------|--------|--------|--------|--------|-----------------|--------|----------------|--------|
| Rock type:                     | Ecl                     |        | Ecl    |        | Amph   |        | Grt-mica schist |        | Grt-Phe schist |        |
|                                | at incl                 | max Mg | rim    | max-P  | core   | rim    | core            | rim    | core           | rim    |
| SiO <sub>2</sub>               | 38.32                   | 38.85  | 38.62  | 39.43  | 38.95  | 38.40  | 37.90           | 37.72  | 38.91          | 38.15  |
| Al <sub>2</sub> O <sub>3</sub> | 21.41                   | 21.40  | 21.63  | 22.02  | 21.90  | 21.39  | 21.33           | 21.27  | 21.80          | 21.34  |
| TiO <sub>2</sub>               | 0.00                    | 0.00   | 0.00   | 0.00   | 0.00   | 0.00   | 0.00            | 0.00   | 0.00           | 0.00   |
| FeO                            | 25.43                   | 22.97  | 24.38  | 17.87  | 24.04  | 26.02  | 28.98           | 30.04  | 24.96          | 27.91  |
| MnO                            | 0.70                    | 0.53   | 1.10   | 0.54   | 0.73   | 1.05   | 0.79            | 1.28   | 0.45           | 1.23   |
| MgO                            | 5.12                    | 6.95   | 5.45   | 7.77   | 7.73   | 6.28   | 4.72            | 4.72   | 8.00           | 4.90   |
| CaO                            | 9.02                    | 9.30   | 8.82   | 12.38  | 6.64   | 6.87   | 6.29            | 4.97   | 5.88           | 6.47   |
|                                | 100.00                  | 100.00 | 100.00 | 100.00 | 100.00 | 100.00 | 100.00          | 100.00 | 100.00         | 100.00 |
|                                | Normalized to 8 cations |        |        |        |        |        |                 |        |                |        |
| Si                             | 2.99                    | 2.99   | 3.00   | 2.99   | 2.99   | 2.98   | 2.98            | 2.98   | 2.99           | 2.99   |
| Al                             | 1.97                    | 1.94   | 1.98   | 1.97   | 1.98   | 1.96   | 1.98            | 1.98   | 1.98           | 1.97   |
| Ti                             | 0.00                    | 0.00   | 0.00   | 0.00   | 0.00   | 0.00   | 0.00            | 0.00   | 0.00           | 0.00   |
| Fe <sup>2+</sup>               | 1.66                    | 1.48   | 1.58   | 1.13   | 1.54   | 1.69   | 1.91            | 1.98   | 1.60           | 1.83   |
| Mn                             | 0.05                    | 0.03   | 0.07   | 0.03   | 0.05   | 0.07   | 0.05            | 0.09   | 0.03           | 0.08   |
| Mg                             | 0.59                    | 0.80   | 0.63   | 0.88   | 0.89   | 0.73   | 0.55            | 0.56   | 0.92           | 0.57   |
| Ca                             | 0.75                    | 0.77   | 0.73   | 1.00   | 0.55   | 0.57   | 0.53            | 0.42   | 0.48           | 0.54   |
|                                | 8.00                    | 8.00   | 8.00   | 8.00   | 8.00   | 8.00   | 8.00            | 8.00   | 8.00           | 8.00   |
| X(Fe)                          | 0.54                    | 0.48   | 0.52   | 0.37   | 0.51   | 0.55   | 0.63            | 0.65   | 0.53           | 0.60   |
| X(Mn)                          | 0.02                    | 0.01   | 0.02   | 0.01   | 0.02   | 0.02   | 0.02            | 0.03   | 0.01           | 0.03   |
| X(Mg)                          | 0.20                    | 0.26   | 0.21   | 0.29   | 0.29   | 0.24   | 0.18            | 0.18   | 0.30           | 0.19   |
| X(Ca)                          | 0.25                    | 0.25   | 0.24   | 0.33   | 0.18   | 0.19   | 0.17            | 0.14   | 0.16           | 0.18   |

<sup>1</sup>Totals are normalized to 100 wt%.

up to 60 cm wide, consisting of garnet, clinopyroxene, and biotite, with up to 3 cm long needles of rutile, occur. Locally, calcite may be present in substantial amounts (up to 10%).

#### *Eclogite*

The eclogite is fine- to medium-grained with granoblastic texture. It consists essentially of garnet (30–40%) and omphacite (50–60%). Rutile, calcite,

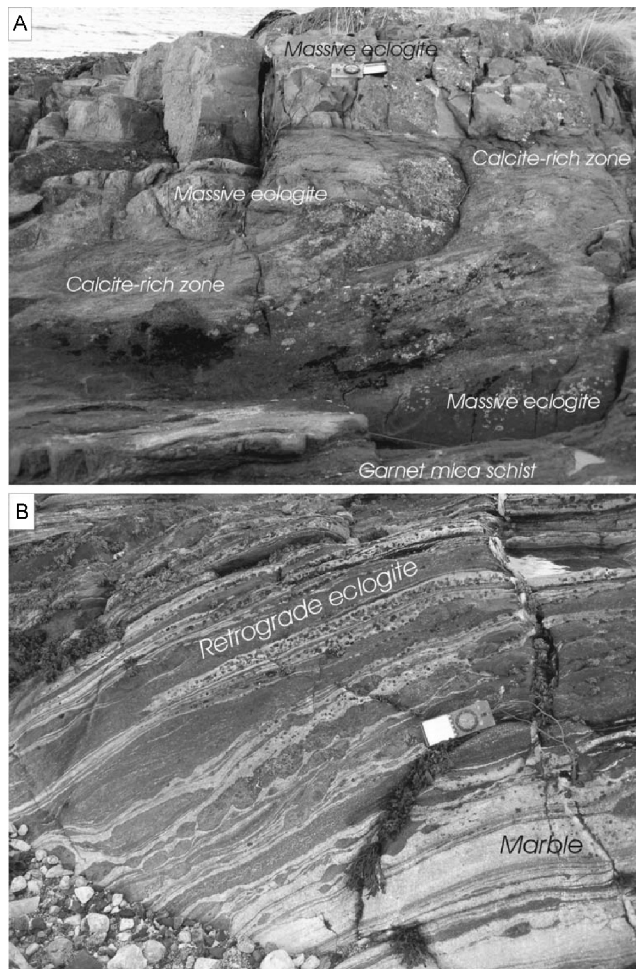


FIG. 3. Field relationships of the Tønsvika eclogite, showing the close association with garnet mica schist and marble.

pyrite, apatite, biotite, and titanite are accessory phases. Garnet locally contains inclusions of pargasite, plagioclase, omphacite, biotite, phengite, paragonite, quartz, rutile, and calcite. Closely spaced amphibole, plagioclase and paragonite occur in certain domains within garnets (Fig. 4A and 4B). In one sample (T-54A3), garnet encloses apparently coexisting albite ( $An_{02-03}$ ) and oligoclase ( $An_{12-15}$ ), together with inclusions of amphibole, paragonite, and quartz (Fig. 4B). Rare omphacite inclusions are present along the garnet rims. Matrix omphacite locally contains inclusions of phengite, rutile, and quartz.

Chemical zoning is locally present in garnets containing inclusions of amphibole and/or plagioclase,

but is otherwise not prominent. In the domains containing amphibole and plagioclase, garnet has a relatively low  $Mg\#$  ( $Mg\# = \frac{100 * Mg}{Mg + Fe^{2+}}$ ),

with an increase toward the rims (Fig. 5A) and a sudden drop at the outermost rim. This zoning pattern is interpreted to represent prograde growth zoning modified by retrograde diffusion along the rims during cooling.

Lath-like symplectite aggregates of biotite + plagioclase in the matrix are interpreted as pseudomorphs after phengite (Fig. 4C). Relict phengite ( $Si_{max} = 6.78$ ) rich in Ti ( $TiO_2 \sim 3.00$  wt%) are preserved as inclusions in garnet (Fig. 4C) and omphacite.

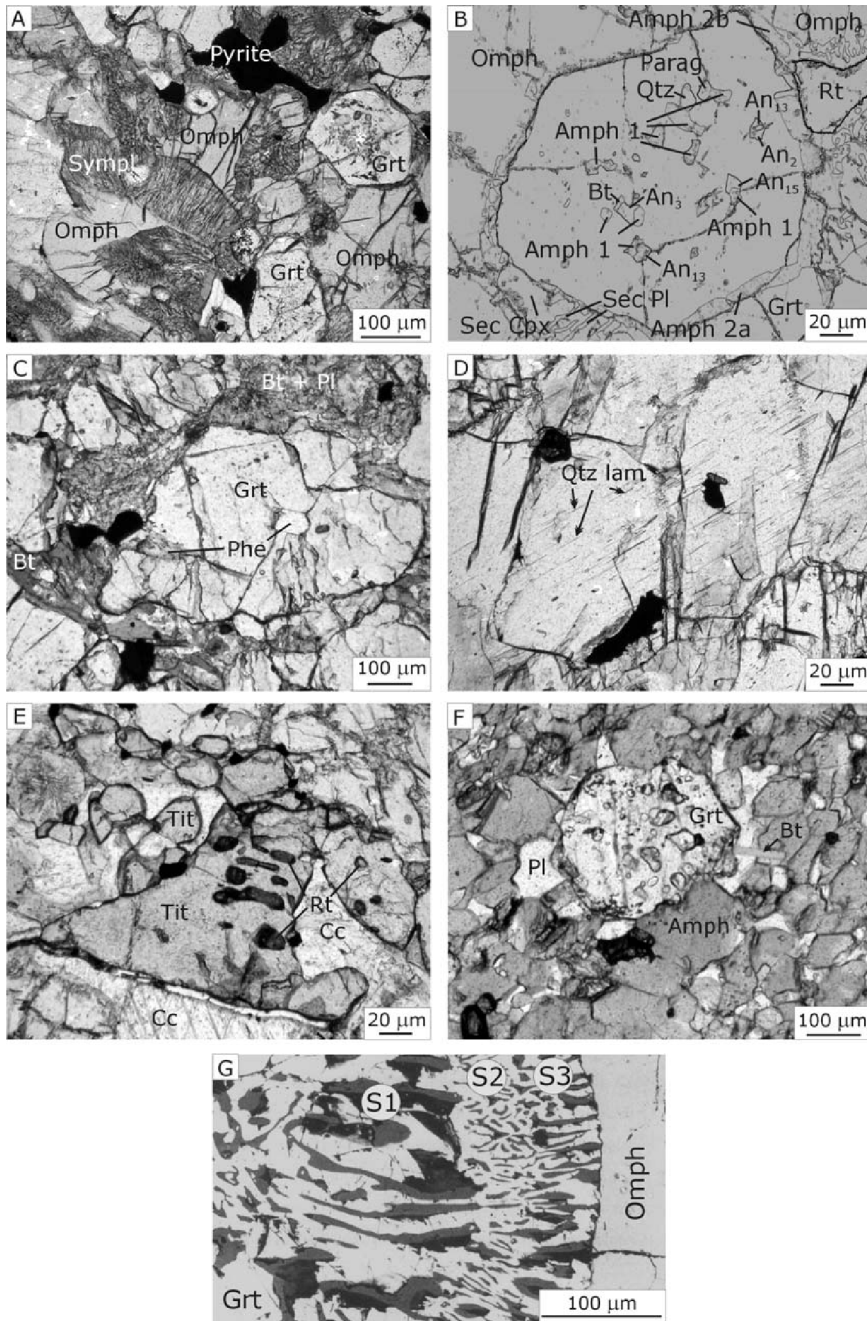


FIG. 4. Textural relationships in eclogite and garnet amphibolite. A. An essentially bimineralec eclogite (sample T-54A3) with garnet and omphacite. Two stages of diopside + plagioclase symplectite can be seen at the center of the image. B. Details of the distribution of solid inclusions garnet (sample T-54A3). Note the appearance of albite and oligoclase in apparent equilibrium. C. Inclusion of high-Si phengite in eclogite garnet (sample T-65). Aggregate of biotite + plagioclase in the matrix after former phengite. D. Omphacite with lamellae of quartz (sample T-64). E. Al-rich titanite overgrowing rutile in a calcite-rich eclogite. F. Coexisting garnet + hornblende + plagioclase in garnet amphibolite (Sample T-68-1). G. Electron backscatter image of three stages of symplectite after omphacite (sample T-54A3).

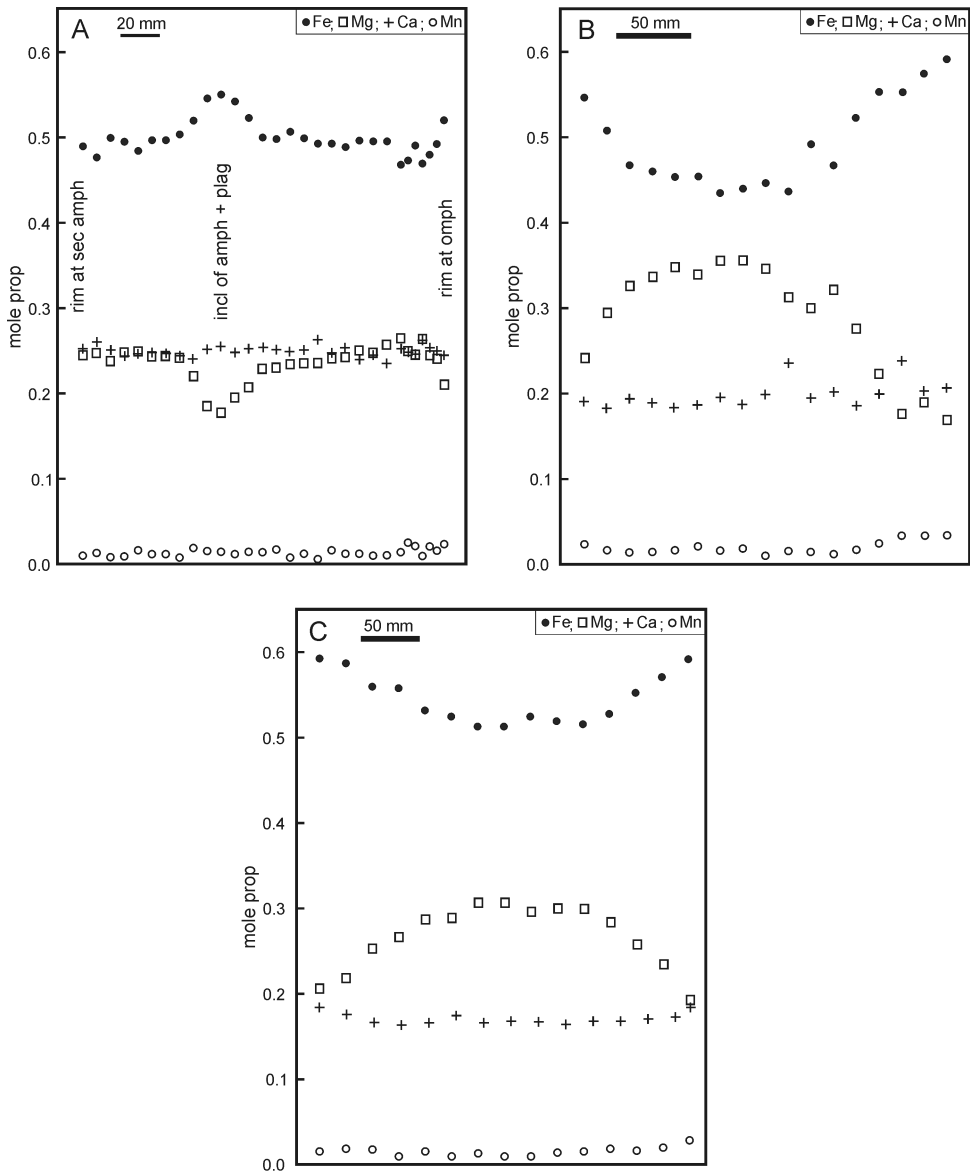


FIG. 5. Zoning profiles of garnet from (A) eclogite (sample T-54A3), (B) garnet amphibolite (sample T-68-1), and (C) garnet mica schist (sample T-41). The amphibolite and mica schist garnets both show evidence of retrograde diffusion zoning, indicating that the cores are relics of the UHP event.

Omphacite ( $X_{Na} = 0.20\text{--}0.40$ ) in the matrix occurs as mosaic textured sub- to anhedral equidimensional grains (0.1–2 mm). Needles of  $\text{SiO}_2$  (quartz) oriented parallel to the (110) cleavage planes (Fig. 4D) are present in some samples, the density being highest within the core of the grains. Partial breakdown of omphacite to symplectitic

intergrowths of plagioclase + diopside is common, and the presence of two generations of symplectite is a general feature (Fig. 4A). Locally, however, three distinct zones of symplectite are observed (Fig. 4G). The spacing of the symplectite lamellae in these three zones is different; the outer zone (S1) has the coarsest lamellae, the intermediate zone (S2) has the

TABLE 3. Selected Clinopyroxene Analyses<sup>1</sup>

| Sample:<br>Rock type:<br>Mineral/stage: | T-54A3 |       |        |       | T-65  |
|-----------------------------------------|--------|-------|--------|-------|-------|
|                                         |        | Ecl   |        |       | Ecl   |
|                                         | omph   | S1    | S2     | S3    | omph  |
| SiO <sub>2</sub>                        | 54.12  | 52.25 | 52.11  | 52.01 | 52.64 |
| Al <sub>2</sub> O <sub>3</sub>          | 8.64   | 6.79  | 5.46   | 4.9   | 6.3   |
| TiO <sub>2</sub>                        | 0.41   | 0.49  | 0.47   | 0.53  | 0.49  |
| FeO                                     | 6.51   | 6.9   | 7.42   | 6.8   | 6.3   |
| MnO                                     | 0      | 0     | 0      | 0     | 0     |
| MgO                                     | 9.69   | 11.52 | 12.42  | 13.2  | 11.97 |
| CaO                                     | 15.29  | 18.73 | 19.71  | 20.4  | 19.11 |
| Na <sub>2</sub> O                       | 5.34   | 3.33  | 2.42   | 2.16  | 3.17  |
| Total                                   | 100    | 100   | 100.01 | 100   | 100   |
| Normalized to 4 cations                 |        |       |        |       |       |
| Si                                      | 1.95   | 1.9   | 1.9    | 1.9   | 1.91  |
| Al(iv)                                  | 0.05   | 0.1   | 0.1    | 0.1   | 0.09  |
| Al(vi)                                  | 0.31   | 0.19  | 0.14   | 0.11  | 0.18  |
| Ti                                      | 0.01   | 0.01  | 0.01   | 0.01  | 0.01  |
| Fe <sup>tot</sup>                       | 0.2    | 0.21  | 0.23   | 0.21  | 0.19  |
| Mn                                      | 0      | 0     | 0      | 0     | 0     |
| Mg                                      | 0.52   | 0.62  | 0.68   | 0.72  | 0.65  |
| Ca                                      | 0.59   | 0.73  | 0.77   | 0.8   | 0.74  |
| Na                                      | 0.37   | 0.23  | 0.17   | 0.15  | 0.22  |
| Total                                   | 4      | 4     | 4      | 4     | 4     |

<sup>1</sup>Totals are normalized to 100 wt%.

finest, and the innermost zone (S3) has intermediate spacing. The symplectites do not appear to be deformed.

Dark green to bluish green kelyphitic rims of hornblende around garnet (Fig. 4B; Amph 2a), and dark green hornblende developed along grain boundaries between garnet and omphacite (Fig. 4B; Amph 2b), are common. Locally diopside in symplectite is partly replaced by greenish hornblende, and large poikilitic hornblende may totally replace the secondary diopside. Aggregates of secondary biotite + plagioclase ± clinozoisite are also seen replacing garnet. All the amphiboles found in eclogite are classified as pargasites (Leake et al., 1997). Inclusions (Amph I) and Amph 2a are most Al-rich (Al(VI) > 1.00). Na(M4) is highest in Amph I (Table 3; Fig. 6).

The amount of calcite varies. It appears as sub-to anhedral grains in matrix and seems to be in textural equilibrium with garnet and omphacite. Rutile (<5%) is common as inclusions in both garnet and omphacite and may occur either as small parallel-aligned, prismatic crystals in the core zone of garnet, or as elongated needles along preferred orientations of ~60/120°. Rutile in matrix may be rimmed by either ilmenite or high- to low-Al titanite (Fig. 4E).

#### Garnet amphibolite

Garnet amphibolite occurs along the recrystallized margins of larger eclogite bodies and as smaller fine-grained greenish black lenses and bands within garnet mica schist and marble. Garnet is concentrated in 4–5 mm wide zones along the



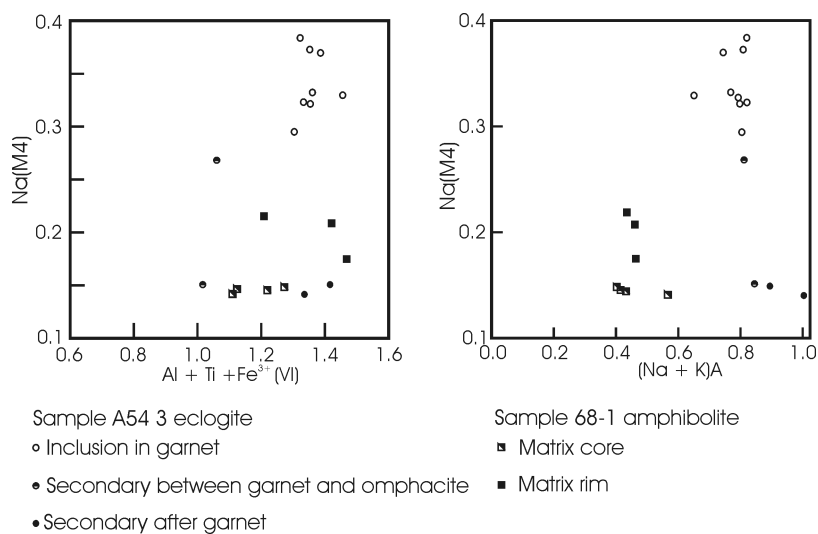


FIG. 6. Chemical variation of amphiboles from some of the metamorphic stages described in the text.

margins of the smaller lenses. The amphibolite locally is strongly aligned parallel to the foliation of the enclosing schist.

The garnet amphibolite consists mainly of greenish hornblende, plagioclase, and garnet in a fine-grained mosaic texture (Fig. 4F), with minor biotite, quartz, clinozoisite, rutile, and titanite. Locally, recrystallized hornblende + plagioclase mimic the preceding symplectite texture from the omphacite breakdown. Hornblende (0.05–0.35 mm) and plagioclase (< 0.1 mm) each comprise up 30–40 % of the rock, whereas idioblastic to subidioblastic garnet (< 0.4 mm) and biotite are each present in amounts of 5–10 %. Hornblende, plagioclase, and garnet are chemically zoned. Garnet cores are chemically similar to the eclogite garnets, showing a typical retrograde diffusion zoning with decreasing Mg# toward the rim (Fig. 5B). Hornblende is classified as tschermakite (Leake et al., 1997), and the Al content increases, whereas the Mg# decreases from core to rim. The Na-content of hornblende in the garnet amphibolite is significantly lower as compared to those occurring in the eclogite (Table 3; Fig. 6). Plagioclase is zoned from An<sub>20</sub> (core) to An<sub>36</sub> (rim). Biotite is unzoned. Rutile occurs as inclusions in garnet and as separate grains in the matrix.

#### Garnet mica schist

Banded mica schist is fine- to medium-grained with a greyish color, commonly with rusty spots after pyrite. Alternating bands consist of mica- and

quartz-rich assemblages. In the mica-rich bands, the biotite/phengite ratio varies, and pure garnet-phengite schist appears locally. Where mafic lenses are embedded in mica-rich rocks, the margins of the mafic rocks have a high content of biotite. The most common variety consists essentially of biotite, phengite, quartz, plagioclase, and garnet. Minor constituents are hornblende, rutile, ilmenite, calcite, and pyrite. Some of the bands are totally devoid of biotite and plagioclase and consist only of garnet + phengite + quartz + rutile. Garnet occurs as idioblastic to sub-idioblastic grains with small commonly parallel-aligned inclusions of quartz, rutile, and biotite. Zoning is displayed by decreasing Mg# from core to rim (Fig. 5C). Phengite cores are rich in Si (6.75–6.80 as a 22 oxygen basis) and Ti (2.10–2.25 wt %). Si shows a marked decrease from core to rim (Table 4). Plagioclase shows increasing An-content (An<sub>19</sub> to An<sub>31</sub>), whereas biotite is virtually unzoned.

#### Marble

Marble is commonly relatively pure, with subordinate amounts of quartz and zoisite. Locally, biotite is present in substantial amounts. Phengite, garnet, rutile and titanite are common accessory phases.

#### P-T Estimates and Metamorphic Evolution

The interpreted metamorphic evolution of the Tønsvika eclogite and associated rocks is based on

TABLE 4. Selected Amphibole Analyses<sup>1</sup>

| Sample:<br>Rock type:          | T-54A3 |                |         | T-68-1 |             |
|--------------------------------|--------|----------------|---------|--------|-------------|
|                                | Amph 1 | Ecl<br>Amph 2a | Amph 2b | Core   | Amph<br>Rim |
| SiO <sub>2</sub>               | 42.4   | 38.79          | 42.94   | 43.68  | 42.92       |
| Al <sub>2</sub> O <sub>3</sub> | 18.12  | 19.78          | 15.24   | 15.43  | 17.34       |
| TiO <sub>2</sub>               | 0.15   | 0.14           | 0.32    | 0.64   | 0.44        |
| FeO                            | 12.12  | 13.45          | 11.51   | 12.32  | 13.05       |
| MnO                            | 0      | 0              | 0       | 0      | 0           |
| MgO                            | 11.38  | 10.59          | 13.3    | 11.95  | 10.74       |
| CaO                            | 9.64   | 11.38          | 10.9    | 11.53  | 11          |
| Na <sub>2</sub> O              | 3.59   | 3.78           | 3.49    | 1.68   | 1.96        |
| K <sub>2</sub> O               | 0.6    | 0.1            | 0.31    | 0.77   | 0.55        |
| Total                          | 98     | 98             | 98      | 98     | 98          |
| Schumacher normalization       |        |                |         |        |             |
| Si                             | 6.14   | 5.68           | 6.21    | 6.31   | 6.2         |
| Al(iv)                         | 1.86   | 2.32           | 1.79    | 1.69   | 1.8         |
| Al(vi)                         | 1.23   | 1.1            | 0.81    | 0.94   | 1.16        |
| Ti                             | 0.02   | 0.02           | 0.04    | 0.07   | 0.05        |
| Fe <sup>3+</sup>               | 0.09   | 0.2            | 0.15    | 0.15   | 0.15        |
| Fe <sup>2+</sup>               | 1.38   | 1.45           | 1.24    | 1.34   | 1.43        |
| Mn                             | 0      | 0              | 0       | 0      | 0           |
| Mg                             | 2.46   | 2.31           | 2.87    | 2.57   | 2.31        |
| Ca                             | 1.5    | 1.79           | 1.69    | 1.79   | 1.7         |
| Na                             | 1.01   | 1.07           | 0.98    | 0.47   | 0.55        |
| K                              | 0.11   | 0.02           | 0.06    | 0.14   | 0.1         |
| Total                          | 15.78  | 15.95          | 15.83   | 15.47  | 15.45       |

<sup>1</sup>Totals are normalized to 98 wt%, and structural formulae calculated according to the calculation scheme of Schumacher (1991).

the micro-textural appearance of different mineral assemblages.

### Subduction

*Stage I—early amphibolite stage.* Preserved inclusions of hornblende + oligoclase + albite + paragonite + quartz in eclogite garnet define an early (pre-eclogite) amphibolite facies stage (stage I). The garnet zoning profile in Figure 5A shows a minimum in Mg# around the entrapped inclusions of hornblende and plagioclase, whereas the Ca content appears to be constant. This is interpreted as representing a relict core of an early garnet growing in equilibrium with the inclusion-suite minerals. The mantle zones of the garnet have a relatively flat

zoning profile with higher Mg#, indicating partial homogenization of the garnet at eclogite-facies conditions. We thus infer that the lowest Mg# represents the most pristine amphibolite-facies garnet composition.

Metamorphic temperatures and pressures for this assemblage were estimated using the garnet-hornblende Fe-Mg thermometers of Perchuk et al. (1985), Powell (1985), and Ravna (2000a), the hornblende-plagioclase thermometer of Holland and Blundy (1994), and the garnet-hornblende-plagioclase-quartz geobarometers of Kohn and Spear (1990). The garnet-hornblende thermometers all give temperatures in the range 585–635°C and, combined with the two barometers (for Mg- and Fe-

TABLE 5. Selected Mica Analyses<sup>1</sup>

| Sample:                        | T-54A3                   |           | T-65       |                 | T-68-2          |                | T-41           |                 |                |
|--------------------------------|--------------------------|-----------|------------|-----------------|-----------------|----------------|----------------|-----------------|----------------|
|                                | Ecl                      |           | Phe in Grt |                 | Grt mica schist |                | Grt+phe schist |                 |                |
| Rock type:                     | Ecl                      |           | Ecl        |                 | Grt mica schist |                | Grt+phe schist |                 |                |
| Mineral:                       | Parag in Grt             | Bt in Grt | Max Si     | Phe matrix core | Phe matrix rim  | Bt matrix core | Bt matr rim    | Phe matrix core | Phe matrix rim |
| SiO <sub>2</sub>               | 47.78                    | 36.41     | 51.27      | 51.52           | 47.87           | 38.2           | 38.82          | 51.12           | 49.57          |
| Al <sub>2</sub> O <sub>3</sub> | 38.17                    | 18.99     | 25.24      | 26.66           | 32.49           | 17.48          | 17.24          | 27.1            | 27.3           |
| TiO <sub>2</sub>               | 0.35                     | 0.69      | 3.08       | 2.12            | 1.44            | 1.73           | 1.51           | 2.26            | 2.55           |
| FeO                            | 0.95                     | 14.21     | 0.96       | 1.76            | 1.5             | 14.72          | 14.47          | 1.38            | 1.9            |
| MnO                            | 0                        | 0         | 0          | 0               | 0               | 0              | 0              | 0               | 0              |
| MgO                            | 0.27                     | 16.31     | 4.33       | 3.37            | 1.73            | 13.94          | 14.01          | 3.24            | 3.21           |
| CaO                            | 0.29                     | 0         | 0          | 0               | 0               | 0              | 0              | 0               | 0              |
| Na <sub>2</sub> O              | 6.83                     | 1.5       | 0.36       | 1.12            | 1.25            | 0.87           | 0.78           | 0.46            | 0.46           |
| K <sub>2</sub> O               | 1.37                     | 7.9       | 10.76      | 9.45            | 9.73            | 9.06           | 9.18           | 10.43           | 11             |
| Total                          | 96                       | 96        | 96         | 96              | 96              | 96             | 96             | 96              | 96             |
|                                | Normalized to 22 oxygens |           |            |                 |                 |                |                |                 |                |
| Si                             | 6.09                     | 5.34      | 6.78       | 6.79            | 6.32            | 5.62           | 5.69           | 6.75            | 6.61           |
| Al(IV)                         | 1.91                     | 2.66      | 1.22       | 1.21            | 1.68            | 2.38           | 2.31           | 1.25            | 1.39           |
| Al(VI)                         | 3.83                     | 0.62      | 2.72       | 2.93            | 3.38            | 0.65           | 0.68           | 2.97            | 2.89           |
| Ti                             | 0.03                     | 0.08      | 0.31       | 0.21            | 0.14            | 0.19           | 0.17           | 0.22            | 0.26           |
| Fe                             | 0.1                      | 1.74      | 0.11       | 0.19            | 0.17            | 1.81           | 1.77           | 0.15            | 0.21           |
| Mn                             | 0                        | 0         | 0          | 0               | 0               | 0              | 0              | 0               | 0              |
| Mg                             | 0.05                     | 3.56      | 0.85       | 0.66            | 0.34            | 3.05           | 3.06           | 0.64            | 0.64           |
| Ca                             | 0.04                     | 0         | 0          | 0               | 0               | 0              | 0              | 0               | 0              |
| Na                             | 1.69                     | 0.43      | 0.09       | 0.29            | 0.32            | 0.25           | 0.22           | 0.12            | 0.12           |
| K                              | 0.22                     | 1.48      | 1.82       | 1.59            | 1.64            | 1.7            | 1.72           | 1.76            | 1.87           |
| Total                          | 13.96                    | 15.9      | 13.9       | 13.87           | 13.99           | 15.65          | 15.62          | 13.86           | 13.99          |

<sup>1</sup>Totals are normalized to 96 wt%.

TABLE 6. Selected Plagioclase Analyses<sup>1</sup>

| Sample:                        | T-54A3      |           |          | T-68-1 |       |       | T-68-2 |       |       |
|--------------------------------|-------------|-----------|----------|--------|-------|-------|--------|-------|-------|
|                                | Olig in grt | Ab in Grt | Eclogite | S2     | S3    | Core  | Rim    | Core  | Rim   |
| Rock type:                     |             |           |          |        |       |       |        |       |       |
| Mineral:                       | Olig in grt | Ab in Grt | Eclogite | S2     | S3    | Core  | Rim    | Core  | Rim   |
| SiO <sub>2</sub>               | 65.86       | 68.48     | 64.73    | 64.27  | 65.02 | 63.79 | 59.93  | 65.49 | 62.63 |
| Al <sub>2</sub> O <sub>3</sub> | 20.66       | 18.85     | 22       | 22.34  | 21.88 | 22.54 | 24.83  | 21.65 | 23.49 |
| Fe <sub>2</sub> O <sub>3</sub> | 0.82        | 0.74      | 0        | 0      | 0     | 0.45  | 0.57   | 0     | 0     |
| CaO                            | 2.37        | 0.28      | 3.18     | 3.77   | 2.92  | 4.18  | 7.35   | 3.76  | 6.27  |
| Na <sub>2</sub> O              | 10.3        | 11.58     | 10.09    | 9.62   | 10.18 | 8.88  | 7.25   | 8.9   | 7.61  |
| K <sub>2</sub> O               | 0           | 0.08      | 0        | 0      | 0     | 0.16  | 0.08   | 0.2   | 0     |
| Total                          | 100         | 100       | 100      | 100    | 100   | 100   | 100    | 100   | 100   |
| Si                             | 2.91        | 3         | 2.85     | 2.84   | 2.86  | 2.83  | 2.68   | 2.91  | 2.8   |
| Al                             | 1.07        | 0.97      | 1.14     | 1.16   | 1.13  | 1.18  | 1.31   | 1.13  | 1.24  |
| Fe <sup>3+</sup>               | 0.03        | 0.02      | 0        | 0      | 0     | 0.02  | 0.02   | 0     | 0     |
| Ca                             | 0.11        | 0.01      | 0.15     | 0.18   | 0.14  | 0.2   | 0.35   | 0.18  | 0.3   |
| Na                             | 0.88        | 0.98      | 0.86     | 0.82   | 0.87  | 0.76  | 0.63   | 0.77  | 0.66  |
| K                              | 0           | 0         | 0        | 0      | 0     | 0.01  | 0      | 0.01  | 0     |
| Total                          | 5           | 5         | 5        | 5      | 5     | 5     | 5      | 5     | 5     |
| X(An)                          | 0.11        | 0.01      | 0.15     | 0.18   | 0.14  | 0.2   | 0.36   | 0.19  | 0.31  |
| X(Ab)                          | 0.89        | 0.98      | 0.85     | 0.82   | 0.86  | 0.79  | 0.64   | 0.8   | 0.69  |
| X(Or)                          | 0           | 0         | 0        | 0      | 0     | 0.01  | 0      | 0.01  | 0     |

<sup>1</sup>Totals are normalized to 100 wt%.

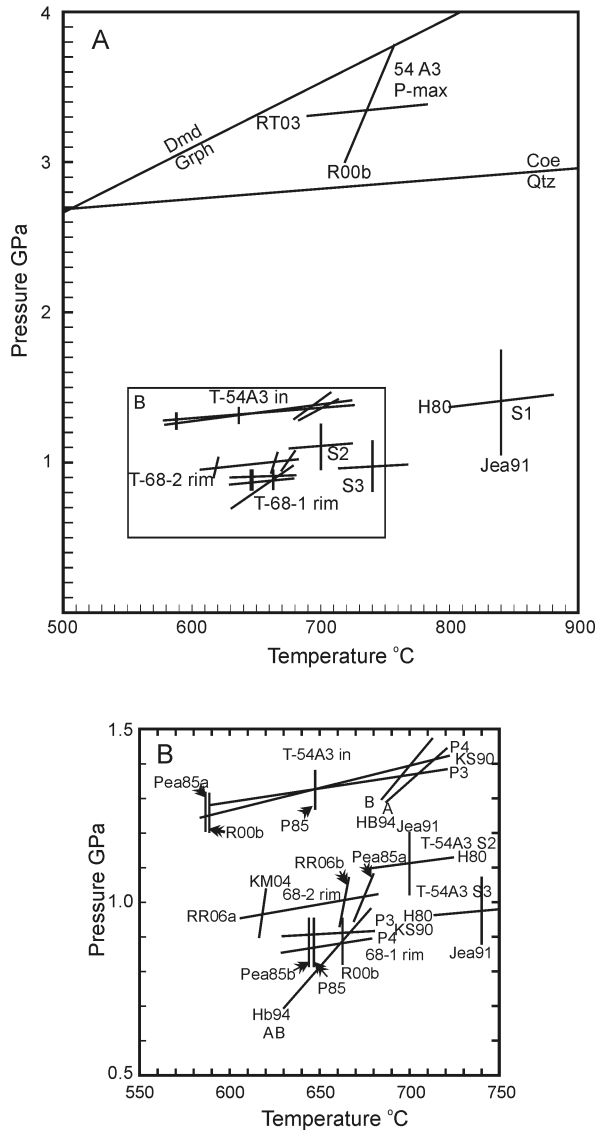


FIG. 7. A. P-T calculations of the various metamorphic stages described in the text. B. Details in the P-T range 0.5–1.5 GPa, 550–750 °C.

end members; Kohn and Spear, 1990), a pressure of ~1.2 GPa. Combinations of the two thermometric expressions of Holland and Blundy (1994) and the two barometric expressions of Kohn and Spear (1990) all intersect close to 700°C/1.38 GPa (Fig. 7). The difference in temperatures obtained by the two different mineral pairs may be related to chemical parameters and/or later thermal overprint. The present amphibole composition is outside the range

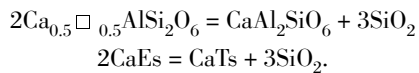
(too high NaM4) for the calibration of the Fe-Mg thermometer of Ravna (2000a) but within the limits used by Perchuk et al. (1985) and the original calibration of Graham and Powell (1984), later revised by Powell (1985). Later thermal overprint could, however, also have affected the Fe-Mg distribution between hornblende and host garnet. Thus the hornblende-plagioclase thermometers, which are expected to be more robust to later overprinting

as they are based on net-transfer reactions, are preferred here. Also, the hornblende composition in the present assemblage is far more sodic than the recommended compositional limits given by Kohn and Spear (1990). The effect of this parameter is uncertain. To conclude, the estimated P-T conditions for stage I are not well established.

*Stage II—eclogite stage.* Stage II is identified by the stable matrix assemblage garnet + omphacite ± phengite ± quartz + rutile ± Al-rich titanite. As mentioned above, matrix phengite is totally decomposed to aggregates of biotite + plagioclase; thus, inclusions of phengite in virtually unzoned garnet and omphacite are regarded as part of the maximum-P stage II assemblage. For thermobarometric calculations of the maximum pressure conditions, we have taken mineral compositions based on the criteria recommended by Ravna and Terry (2004; maximum Si content in phengite, maximum Jd content in omphacite and maximum

$a_{pyr}^{Grt} * (a_{grs}^{Grt})^2$  in garnet). A combination of the garnet-clinopyroxene Fe-Mg thermometer of Ravna (2000b) and the garnet-clinopyroxene-phengite barometer of Ravna and Terry (2004) intersects at 735°C/3.36 GPa, well into the coesite stability field (Fig. 7), thus presenting the Tromsø Nappe as a new possible candidate for the UHPM family. Any retrograde resetting of the mineral compositions would bring the pressure estimates to lower values.

Abundant, parallel-oriented needle-like inclusions of pure SiO<sub>2</sub> in omphacite may be exsolution features. The presence of clinopyroxene with oriented quartz needles in several UHP terranes (e.g. Smith, 1984; Katayama et al., 2000) has led to a general conclusion that CaEs-bearing pyroxene is stable only at UHP conditions. However, reversed experiments by Gasparik (1986) show that CaEs-bearing pyroxene also is stable well into the quartz stability field. This issue has been discussed by Page et al. (2005), who present evidence for quartz + amphibole exsolution in omphacite from HP eclogites in the Eastern Blue Ridge, southern Appalachians, United States. They concluded that the presence of a diluted (5–10 %) CaEs component in clinopyroxene does not require UHP conditions. In the Tønsvika eclogite, neither amphibole nor other minerals have been detected along the quartz rods in the omphacite, indicating that exsolution was from an earlier omphacite enriched in the Ca-Eskola molecule after the reaction (Smyth, 1980):



However, we regard the status of the omphacite with exsolved quartz rods as uncertain.

### Decompression

*Stage III—symplectite stages.* The post-eclogite decompression is well documented within the present eclogites, the most striking feature being the decomposition of omphacite to symplectitic intergrowths of diopside + plagioclase. Most of the studied samples show two distinct zones of symplectite breakdown, whereas three stages have been documented in one sample (54A3). These have been denoted as stages S1, S2, and S3 (Table 1). According to Joanny et al. (1991), the phase transition omphacite to Ca-clinopyroxene + plagioclase can be classified as a discontinuous precipitation reaction. The lamellar spacing (L) is thus a function of temperature according to the growth law

$$\log L = A - BT,$$

where A and B are constants. On this basis, Joanny et al. (1991) were able to construct an empirical geothermometer as a function of the spacing of symplectitic lamellae. We have used this method to estimate the formation temperature for the three lamellar symplectite stages in sample 54A3. As the accuracy of this method is strongly dependent on how we measure the width of the lamellae, we have made our measurements on the thinnest and best-preserved lamellae as close to the reaction front as possible to reduce the uncertainties of the cutting effect and other effects, according to the recommendations of Joanny et al. (1991). The results are summarized in Table 1, and calculations give a temperatures of 840 ± 50°C for S1, 700 ± 50°C for S2, and 740 ± 50°C for S3. Pressure estimates for the three symplectitic stages can be obtained from the compositions of clinopyroxene and plagioclase in each of them using the jadeite-in-clinopyroxene coexisting with plagioclase barometer of Holland (1980). S1 gives 1.41 GPa at 840°C, S2 1.12 GPa at 700°C, and S3 0.98 GPa at 740°C (Fig. 7).

Fluid inclusions in omphacite could contribute to the presence of a fluid phase during the symplectite-forming events. This will greatly enhance the diffusion rate, and thus increase the width of the lamellae. A possible effect of such fluids can not be excluded. It is, however, not realistic to suggest that

TABLE 7. Calculated P-T Values Based on Various Geothermobarometers

| Sample | Rock type       | Stage  | P GPa    | T°C     | Methods                     |
|--------|-----------------|--------|----------|---------|-----------------------------|
| T-54A3 | Eclogite        | I      | 1.2      | 585–635 | Pea85a, P85, R00a + KS90    |
|        |                 | I      | 1.38     | 700     | HB94 + KS90                 |
| T-65   | Eclogite        | II     | 3.36     | 735     | R00b + RT03                 |
| T-54A3 | Eclogite        | III S1 | 1.41     | 840     | Jea91 + H80                 |
|        |                 | III S2 | 1.12     | 700     | Jea91 + H80                 |
|        |                 | III S3 | 0.98     | 740     | Jea91 + H80                 |
| T-68-1 | Grt-amphibolite | IV     | 0.91     | 660     | Pea85a, P85, R00a + KS90    |
| T-68-1 | Grt-amphibolite | IV     | 0.91     | 660     | HB94 + KS90                 |
| T-68-2 | Grt-mica schist | IV rim | 1.0–1.06 | 675     | Pea85b, KM04, RR06b + RR06a |

<sup>1</sup>Thermometers: Pea85a = Perchuk et al., 1985; P85 = Powell, 1985; R00a = Ravna, 2000a (garnet-hornblende Fe-Mg); R00b = Ravna, 2000b (garnet-clinopyroxene Fe-Mg); HB94 = Holland and Blundy, 1994 (hornblende-plagioclase); Jea91 = Joanny et al., 1991 (symplectite lamellae spacing); Pea85b = Perchuk et al., 1985; KM04 = Kaneko and Miyano, 2004, 2005 (garnet-biotite); RR06b = this paper (garnet-biotite Fe-Mg). Barometers: KS90 = Kohn and Spear, 1990 (garnet-hornblende-plagioclase-quartz); RT03 = Ravna and Terry, 2004 (garnet-clinopyroxene-phengite); H80 = Holland, 1980 (albite in clinopyroxene); RR06a = this paper (garnet-biotite-muscovite-plagioclase-quartz).

this could have affected the three stages independently of each other—all three stages should have been equally affected and the relative width of the lamellae would have been the same. Furthermore, at the estimated P-T conditions for stage S2 and S3, an H<sub>2</sub>O-rich fluid phase would probably have caused extensive amphibolitization of the symplectite domains.

*Stage IV—amphibolite stage.* Hydration and recrystallization within amphibolite facies conditions is well expressed along the well-foliated margins of more massive eclogite lenses and in thinner bands within garnet mica schist and marble. The stable assemblage is garnet + hornblende + plagioclase + quartz ± biotite + rutile. Garnet cores have a composition that reflects that they are remnants of the earlier eclogite facies, with relatively high Mg# relative to the rim. Also, hornblende and plagioclase show zoning that can be related to a pressure decrease, with plagioclase showing a distinct increase in anorthite from An<sub>21</sub> (core) to An<sub>35</sub> (rim). The core composition of the garnet was most probably not in equilibrium with core compositions of either hornblende or plagioclase. Attempts to estimate P-T conditions on core compositions have therefore not been made. Application of the Powell (1985), Perchuk et al. (1985), and Ravna (2000a) garnet-hornblende Fe-Mg thermometers on rim

compositions all yield similar temperatures of 650–670°C. A combination of the Holland and Blundy (1994) hornblende-plagioclase thermometers and the Kohn and Spear (1990) barometers intersect tightly at ~660°C, 0.91 GPa (Fig. 7). Thus, all available thermometric methods give identical results.

In the garnet mica schist, the assemblage garnet + biotite + phengite + plagioclase + quartz can give both temperature and pressure. The garnet-biotite-muscovite-plagioclase geobarometer (linear expression derived from THERMOCALC; Powell and Holland, 1988—see appendix) have been used in combination with various versions of the garnet-biotite Fe-Mg thermometer. Thermometers used are Perchuk et al. (1985) and Kaneko and Miyano (2004, 2005). In addition we have combined the Ferry and Spear (1978) calibration of the garnet-biotite thermometer with the empirical  $\ln K_D$  vs.  $(S_{ca} + X_{Mn})^{Grt}$  relationship shown for garnet-biotite pairs from the Tromsø Nappe (Krogh et al., 1990) to retrieve a new thermometric expression:

$$T(^{\circ}C) = \frac{2089 + 1403.5*(X_{Ca} + X_{Mn})^{Grt} + 95.6*P(GPa)}{\ln K_D + 0.782} - 273$$

The results are given in Table 7. As in the garnet amphibolite, cores of garnet, biotite, phengite, and

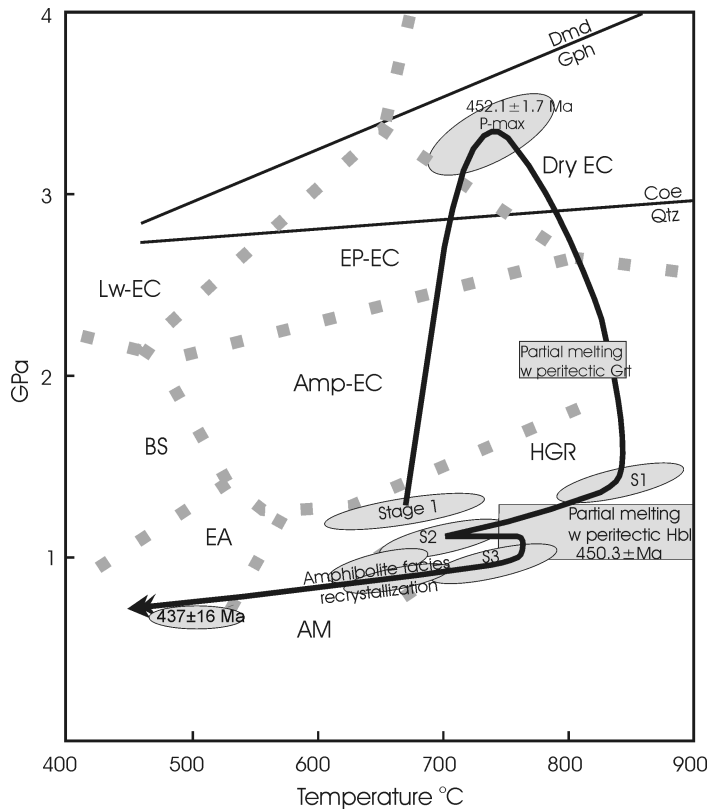


FIG. 8. P-T-t path for the Tønsvika eclogite based on P-T calculations on various mineral assemblages (this paper), data on partial melting (Stevenson, 2005, pers. com.), and age data from Krogh et al. (1990) and Corfu et al. (2003).

plagioclase were probably never in equilibrium, inasmuch as plagioclase obviously was absent during the highest pressures. The cores of phengite in garnet mica schist and garnet phengite schist are probably relics of the maximum-P stage, as their high-Si content is equal to that in the phengite included in eclogite garnet. Core compositions have thus not been used for thermobarometry in the garnet mica schist. Rim compositions give results in the range 620 to 677°C and 1.0 to 1.06 GPa, the recently calibrated garnet-biotite thermometer of Kaneko and Miyano (2004, 2005) yielding the lowest temperature. This thermometer is, however, only calibrated for fairly low Ca garnets ( $X_{Ca} = 0-0.07$ ), whereas the Ca-content of garnet in sample T-68-2 is substantially higher ( $X_{Ca} = 0.15$ ). The other two expressions give temperatures that are comparable with the garnet-hornblende (Perchuk et al., 1985; Powell, 1985; Ravna, 2000a) Fe-Mg thermometers

as well as the hornblende-plagioclase thermometers (Holland and Blundy, 1994).

The P-T estimates for the different metamorphic stages and the metamorphic evolution for the Tønsvika eclogite and associated rocks are summarized in Figures 7A and 7B, which give a detailed P-T path for the post-eclogite evolution (Fig. 8).

## Discussion

The present data provide good evidence for prograde subduction-related metamorphism of the Tromsø Nappe, in accordance with previous data presented by Krogh et al. (1990) and Ravna et al. (2006). Maximum pressures calculated for the Tønsvika eclogite are well within the coesite stability field, indicating that these rocks reached UHP conditions. However, so far, no indication of either coesite or polycrystalline quartz aggregates have



been identified, which makes the UHP nature of the present rocks disputable. The most robust and reliable petrographical evidence is thus absent, and only indirect evidence can be used. The reliability of the garnet-clinopyroxene-phengite geobarometer to discriminate between HP and UHP eclogites has been shown by Ravna and Terry (2004). Application of the barometer to a variety of HP and UHP eclogites representing a large span in mineral chemistry and P-T conditions has shown that the method is capable, within uncertainty limits, to place well-documented UHP eclogites within the coesite stability field, whereas typical HP eclogites fall within the quartz stability field (Ravna and Terry, 2004). Gilotti and Ravna (2002) used the method to suggest UHP metamorphism within the North-East Greenland eclogite province (NEGEP) without any firm evidence for the presence of coesite or any other petrographical UHP indicators. Recently, the UHP nature of these eclogites was confirmed by the discovery of coesite inclusions in zircon (Gilotti, 2005, pers. com.).

One common feature of the several hundred eclogite samples examined so far from the Tromsø Nappe is that matrix phengite invariably is absent. The common occurrence of lath-like aggregates of biotite + plagioclase, apparently pseudomorphs after primary phengite, indicates, however, that phengite was a widespread matrix mineral. In a few samples, relict phengite inclusions are preserved in garnet and omphacite. Partial decompression melting is also a common phenomenon in the eclogites; Stevenson (2005) has described two separate events at different P-T conditions post-dating the maximum P stage of the rocks. This indicates that post-max-P heating was an important factor during the early uplift stages of the subducted sequence, thus minimizing the chances for coesite preservation. The temperature increase would enhance the back-reaction rate of coesite to quartz, and also the recrystallization of any polycrystalline quartz aggregates included in garnet or omphacite. The heat source for the thermal peak estimated for symplectite stage S3 and the apparently coeval partial melting of eclogite with production of melt + peritectic amphibole, dated to  $450 \pm 0.9$  Ma, most probably was the tectonic juxtaposition of the UHPM Tromsø Nappe rocks and the high-T Skattøra Migmatite Complex (SMC). The SMC was migmatized at  $\sim 1.0$  GPa and  $900^\circ\text{C}$  (Selbekk and Skjerlie, 2002) at  $456 \pm 4$  Ma (Selbekk et al., 2000). The chances to preserve direct or indirect petrographic evidence for the

former presence of coesite would thus be minimal in such a setting. Thus far we have to rely on the available geothermobarometers (Ravna, 2000b; Ravna and Terry, 2004), which in our case clearly indicate UHP metamorphism. Our conclusion on this basis is that the Tromsø Nappe did indeed experience UHP metamorphism.

The Tromsø Nappe and the underlying Nakkedal Nappe Complex (Fig. 1), making up the Uppermost Allochthon of the Scandinavian Caledonides, rests tectonically on top of Silurian metasediments deposited directly on the Lyngen Magmatic Complex (both part of the Upper Allochthon). A U-Pb zircon age obtained from a deformed tonalite dike within the complex, yields  $469 \pm 5$  Ma (Oliver and Krogh, 1995). The Lyngen Magmatic Complex represents oceanic fragments obducted on the margin of the Baltic continent in Ordovician (Taconic) time (Pedersen et al., 1988, 1991), at the same time as the Tromsø Nappe rocks were subducted to  $\sim 100$  km depth (Corfu et al., 2003), and the Skattøra Migmatite Complex underwent extensive melting (Selbekk et al., 2000; Selbekk and Skjerlie, 2002).

The rock units of the Uppermost Allochthon are believed to represent fragments of the Laurentian continental margin (Stephens and Gee, 1985, 1989; Roberts et al., 1985; 2001; 2002; Yoshinobu et al., 2002; Roberts, 2003), and may thus be related to the NEGEP (Gilotti, 1994; Gilotti and Elvevold, 1998; Elvevold and Gilotti, 2000; Gilotti and Ravna, 2002). Dating of the North-East Greenland eclogites has, however, yielded Devonian ages of  $\sim 400$  Ma for HP metamorphism in the western and central blocks, similar to the ages of the Western Gneiss Region of southern Norway (Krogh et al., 1974; Carswell et al., 2003), and as young as Carboniferous age ( $360 \pm 5$  Ma; U-Pb zircon) for the UHP metamorphism in the eastern block of the NEGEP (Brueckner et al., 1998; Gilotti et al., 2004). There is therefore no straightforward relationship between the Tromsø and North-East Greenland eclogites. Eclogites of similar (Taconic) age to the Tromsø eclogites are reported from Biscayerhalvøya, Svalbard (Gee and Gromet, 1998) and the eastern Blue Ridge of North Carolina ( $\sim 460$  Ma; Miller et al., 2000). This Taconian link has been pointed out by Steltenpohl et al. (2003), who also suggested that eclogites within shear zones in the Lofoten igneous province (Kullerud et al., 2001; Markl and Bucher, 1997) are of the same age.

The exhumation of the Tromsø Nappe rocks appears to have been rapid, as evidenced by the

dating of Corfu et al. (2003) and the P-T data presented here. Maximum pressures within the coesite stability field (3.36 GPa at 735°C) apparently were reached at  $452.1 \pm 1.7$  Ma, whereas partial melting involving peritectic hornblende at 1.0–1.2 GPa was attained at  $450.3 \pm 0.9$  Ma (Corfu et al., 2003). These data are similar to those given for the early exhumation of the Dora Maira (Rubatto and Hermann, 2001). Using the approach regarding lithostatic pressures vs. depth given by Rubatto and Hermann (2001), a mean exhumation rate of 3.6 cm/yr (36 km/m.y.) is obtained for the early Tromsø Nappe rocks, compared to 3.4 cm/year for Dora Maira.

### Summary

The eclogitic rocks from the Tromsø Nappe show a complex metamorphic history, giving well-documented evidence of prograde subduction-related evolution. The maximum pressure estimate presented in this paper indicates that UHP conditions were reached. The post-eclogite P-T evolution of the present rocks based on textural observations and thermobarometry indicate a moderate increase in T to >800°C during the initial phases of uplift from 3.36 GPa to ~1.4 GPa (Fig. 8), succeeded by cooling at further uplift, and then by an event of approximately isobaric heating before final cooling and decompression. This is in line with the observed appearance of two separate stages of partial decompression melting observed in eclogites from the area, the oldest involving peritectic garnet occurring at 2.0–2.2 GPa, 762–844°C and the youngest involving peritectic hornblende at 1.0–1.3 GPa, 743–950°C (Stevenson, 2005). Initial uplift was rapid, estimated at ~3.6 cm/y.

A summary based on the observed textural observations and geothermobarometric estimates as given in Figure 8, and additional data from Stevenson (2005), is presented below.

1. Stage I is represented by hornblende + plagioclase (albite + oligoclase) + paragonite + biotite + quartz included in garnet. Estimated P-T conditions are 1.4 GPa/675°C.

2. During Stage II, maximum P-T conditions for eclogites give UHP conditions of up to 3.36 GPa at 735°C.

3. Early post-max-P conditions pass through conditions where partial melting of eclogites involving peritectic garnet is formed at 2.0–2.2 GPa and 760–845°C (Stevenson, 2005).

4. Attending Stage III, three stages of symplectite formation (S1, S2, and S3) are recognized, apparently being formed at 1.41 GPa/840°C, 1.12 GPa/700°C, and 0.98 GPa/750°C, respectively. The partial melting involving peritectic hornblende (Stevenson, 2005) may be related to the temperature increase observed for stage S3 and the tectonic coupling of the Tromsø Nappe rocks with the hot Skattøra Migmatite Complex.

5. The tectonic juxtaposition of the Tromsø Nappe and the Skattøra Migmatite Complex caused strong ductile deformation and recrystallization of the involved rocks as temperatures cooled off into the amphibolite-facies regime (Stage IV).

### Acknowledgments

We wish to acknowledge Dr. Synnøve Elvevold, Norwegian Polar Institute, for a thorough review of the paper; Associate Professor G. C. Corner, Department of Geology, University of Tromsø for cleaning up the language; and T. I. Eilertsen, Laboratory of Electron Microscopy, University of Tromsø for maintaining the analytical equipment at a high standard.

### REFERENCES

- Bruceckner, H. K., Gilotti, J., and Nutman, A. P., 1998, Caledonian eclogite facies metamorphism of early Proterozoic protoliths from the North-East Greenland Eclogite Province: Contributions to Mineralogy and Petrology, v. 130, p. 103–120.
- Carswell, D. A., Bruceckner, H. K., Cuthbert, S. J., Metha, K., and O'Brien, P. J., 2003, The timing of stabilisation and the exhumation rate for ultra-high pressure rocks in the Western Gneiss Region of Norway: Journal of Metamorphic Geology, v. 21, p. 601–612.
- Carswell, D. A., and Compagnoni, R., 2003, Introduction with review of the definition, distribution, and geotectonic significance of ultrahigh pressure metamorphism, in Carswell, D. A., and Compagnoni, R., eds., Ultrahigh pressure metamorphism: EMU notes in Mineralogy, v. 5, p. 3–9.
- Corfu, F., Ravna, E. J. K., and Kullerød, K., 2003, A late Ordovician U-Pb age for the Tromsø Nappe eclogites, Uppermost Allochthon of the Scandinavian Caledonides: Contributions to Mineralogy and Petrology, v. 145, p. 502–513.
- Dallmeyer, R. D., and Andresen, A., 1992, Polyphase tectonothermal evolution of exotic Caledonian nappes in Troms, Norway: Evidence from  $^{40}\text{Ar}/^{39}\text{Ar}$  mineral ages: Lithos, v. 29, p. 19–42.
- Elvevold, S., and Gilotti, J. A., 2000, Pressure-temperature evolution of retrogressed kyanite eclogites,

- Weinschenk Island, North-East Greenland Caledonides: *Lithos*, v. 53, p. 127–147.
- Ferry, J. M., and Spear, F. S., 1978, Experimental calibration of partitioning of Fe and Mg between biotite and garnet: *Contributions to Mineralogy and Petrology*, v. 66, p. 113–117.
- Ganguly, J., Cheng, W., and Tirone, M., 1996, Thermodynamics of aluminosilicate garnet solid solution: New experimental data, an optimized model, and thermometry applications: *Contributions to Mineralogy and Petrology*, v. 126, p. 137–151.
- Gasparik, T., 1986, Experimental study of subsolidus phase relations and mixing properties of clinopyroxene in the silica saturated system  $\text{CaO-MgO-Al}_2\text{O}_3\text{-SiO}_2$ : *American Mineralogist*, v. 71, p. 686–693.
- Gee, D. G., and Gromet, L. P., 1998, An evaluation of the age of high-grade metamorphism in the Caledonides of Biscayerhalvøya, NW Svalbard: *Geologiska Föreningens Förhandlingar*, v. 120, p. 199–208.
- Ghent, E. D., and Stout, M. Z., 1981, Geobarometry and geothermometry of plagioclase-biotite-garnet-muscovite assemblages: *Contributions to Mineralogy and Petrology*, v. 76, p. 92–97.
- Gilotti, J. A., 1994, Eclogites and related high-pressure rocks from North-East Greenland: Rapport fra Grønlands Geologiske Undersøgelse, v. 162, p. 77–90.
- Gilotti, J. A., and Elvevold, S., 1998, Partial eclogitization of the Ambolten gabbro-norite, North-East Greenland Caledonides: *Schweizerische Mineralogische und Petrographische Mitteilungen*, v. 78, p. 273–292.
- Gilotti, J. A., Nutman, A. P., and Brueckner, H. K., 2004, Devonian to Carboniferous collision in the Greenland Caledonides: U-Pb zircon and Sm-Nd ages of high-pressure and ultrahigh-pressure metamorphism: *Contributions to Mineralogy and Petrology*, v. 148, p. 216–235.
- Gilotti, J. A., and Ravna, E. J. K., 2002, First evidence for ultrahigh-pressure metamorphism in the North-East Greenland Caledonides: *Geology*, v. 30, p. 551–554.
- Graham, C. M., and Powell, R., 1984, A garnet-hornblende geothermometer: Calibration, testing, and application to the Pelona Schist, Southern California: *Journal of Metamorphic Geology*, v. 2, p. 13–31.
- Holland, T. J. B., 1980, Reaction albite = jadeite + quartz determined experimentally in the range 600–1200°C: *American Mineralogist*, v. 65, p. 129–134.
- Holland, T., and Blundy, J., 1994, Non-ideal interactions in calcic amphiboles and their bearing on amphibole-plagioclase thermometry: *Contributions to Mineralogy and Petrology*, v. 116, p. 433–447.
- Holland, T., and Powell, R., 1992, Plagioclase feldspars—activity-composition relations based upon Darken quadratic formalism and Landau theory: *American Mineralogist*, v. 77, p. 53–61.
- Holland, T. J. B., and Powell, R., 1998, An internally consistent thermodynamic data set for phases of petrological interest: *Journal of Metamorphic Geology*, v. 16, p. 309–343.
- Joanny, V., van Roermund, H., and Lardeaux, J.-M., 1991, The clinopyroxene/plagioclase symplectite in retrograde eclogites: A potential geothermobarometer: *Geologische Rundschau*, v. 80, p. 303–320.
- Kaneko, Y., and Miyano, T., 2004, Recalibration of mutually consistent garnet-biotite and garnet-cordierite geothermometers: *Lithos*, v. 73, p. 255–269.
- Kaneko, Y., and Miyano, T., 2005, Erratum to “Recalibration of mutually consistent garnet-biotite and garnet-cordierite geothermometers” (*Lithos*, v. 73, p. 255–269): *Lithos* [doi: 10.1016/j.lithos.2005.09.003].
- Katayama, I., Parkinson, C. D., Okamoto, K., Nakajima, Y., and Maruyama, S., 2000, Supersilicic clinopyroxene and silica exsolution in UHPM eclogite and pelitic gneiss from the Kokchetav massif, Kazakhstan: *American Mineralogist*, v. 85, p. 1368–1374.
- Kohn, M. J., and Spear, F. S., 1990, Two new geobarometers for garnet amphibolites, with applications to southeastern Vermont: *American Mineralogist*, v. 75, p. 89–96.
- Krogh, E. J., Andresen, A., Bryhni, I., Broks, T. M., and Kristensen, S. E., 1990, Eclogites and polyphase P-T cycling in the Caledonian Uppermost Allochthon in Troms, northern Norway: *Journal of Metamorphic Geology*, v. 8, p. 289–309.
- Krogh, T. E., Mysen, B. O., and Davis, G. L., 1974, A Palaeozoic age for the primary minerals of a Norwegian eclogite: *Carnegie Institute Washington Yearbook*, v. 73, p. 575–576.
- Kullerød, K., Flaatt, K., and Davidsen, B., 2001, High-pressure fluid-rock reactions involving Cl-bearing fluids in lower-crustal ductile shear zones of the Flakstadøy basic complex, Lofoten, Norway: *Journal of Petrology*, v. 42, p. 1349–1372.
- Leake, B. E., Wolley, A. R., Arps, C. E. S., Birch, W. D., Gilbert, M. C., Grice, J. D., Hawthorne, F. C., Kato, A., Kisch, H. J., Krivovichev, V. G., Linthout, K., Laird, J., Mandarino, J. A., Maresch, W. V., Nickel, E. H., Rock, N. M. S., Schumacher, J. C., Smith, D. C., Stephenson, N. C. N., Ungaretti, L., Whittaker, E. J. W., and Youzhi, G., 1997, Nomenclature of amphiboles: Report of the Subcommittee on Amphiboles of the International Mineralogical Association, Commission on New Minerals and Mineral Names: *American Mineralogist*, v. 82, p. 1019–1037.
- Markl, G., and Bucher, K., 1997, Proterozoic eclogites from the Lofoten islands, northern Norway: *Lithos*, v. 42, p. 15–35.
- Miller, B. V., Stewart, K. G., Miller, C. F., and Thomas, C. W., 2000, U-Pb ages from the Bakersville, North Carolina eclogite: Taconian eclogite metamorphism followed by Acadian and Alleghanian cooling [abs.]: *Geological Society of America, Abstracts with Programs, Southeastern Section*, 2, A-62.

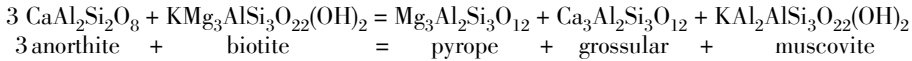
- Oliver, G. J. H., and Krogh, T. E., 1995, U-Pb zircon age of  $469 \pm 5$  Ma for the Kjoslen unit of the Lyngen magmatic complex, northern Norway: *Norges Geologiske Undersøkelse Bulletin*, v. 428, p. 27–33.
- Page, F. Z., Essene, E. J., and Mukasa, S. B., 2005, Quartz exsolution in clinopyroxene is not proof of ultrahigh pressures: Evidence from eclogites from the Eastern Blue Ridge, Southern Appalachians, U.S.A.: *American Mineralogist*, v. 90, p. 1092–1099.
- Pedersen, R. B., Furnes, H. and Dunning, G. R., 1988, Some Norwegian ophiolite complexes reconsidered: *Norges Geologiske Undersøkelse, Special Publications*, v. 3, p. 80–85.
- Pedersen, R. B., Furnes, H., and Dunning, G. R., 1991, A U/Pb age for the Sulitjelma Gabbro, north Norway: Further evidence for the development of a Caledonian marginal basin in Ashgill-Llandovery time: *Geological Magazine*, v. 128, p. 141–153.
- Perchuk, L. L., Aranovich, L. Ya., Podlesskii, K. K., Lavrent'eva, I. V., Gerasimov, V. Yu., Fed'kin, V. V., Kitsul, V. I., Karsakov, L. P., and Berdnikov, N. V., 1985, Precambrian granulites of the Aldan shield, eastern Siberia, USSR: *Journal of Metamorphic Geology*, v. 3, p. 265–310.
- Powell, R., 1985, Regression diagnostics and robust regression in geothermometer/geobarometer calibration: The garnet-clinopyroxene geothermometer revisited: *Journal of Metamorphic Geology*, v. 3, p. 327–342.
- Powell, R., and Holland, T. J. B., 1988, An internally consistent thermodynamic dataset with uncertainties and correlations: 3. Applications to geobarometry, worked examples and a computer program: *Journal of Metamorphic Geology*, v. 6, p. 173–204.
- Ravna, E. J. K., 2000a, Distribution of  $\text{Fe}^{2+}$  and Mg between coexisting garnet and hornblende in synthetic and natural systems: An empirical calibration of the garnet-hornblende Fe-Mg geothermometer: *Lithos*, v. 53, p. 265–277.
- Ravna, E. J. K., 2000b, The garnet-clinopyroxene geothermometer—an updated calibration: *Journal of Metamorphic Geology*, v. 18, p. 211–219.
- Ravna, E. J. K., Kullerud, K., and Ellingsen, E., 2006, Prograde garnet-bearing ultramafic rocks from the Tromsø Nappe, Northern Scandinavian Caledonides: *Lithos*, in press [doi: 10.1016/j.lithos.200603.058].
- Ravna, E. J. K., and Terry, M. P., 2004, Geothermobarometry of UHP and HP eclogites and schists—an evaluation of equilibria among garnet-clinopyroxene-kyanite-phengite-coesite/quartz: *Journal of Metamorphic Geology*, v. 22, p. 579–592.
- Roberts, D., 2003, The Scandinavian Caledonides: Event chronology, palaeogeographic settings, and likely modern analogues: *Tectonophysics*, v. 365, p. 283–299.
- Roberts, D., Heldal, T., and Melezhik, V. M., 2001, Tectonic structural features of the Fauske conglomerates in the Løvgavlen quarry, Nordland, Norwegian Caledonides, and regional implications: *Norsk Geologisk Tidsskrift*, v. 81, p. 245–256.
- Roberts, D., Melezhik, V. M., and Heldal, T., 2002, Carbonate formations and NW-directed thrusting in the highest allochthons of the Norwegian Caledonides: Evidence of a Laurentian ancestry: *Journal of the Geological Society of London*, v. 159, p. 117–120.
- Roberts, D., Sturt, B. A., and Furnes, H., 1985, Volcanite assemblages and environments in the Scandinavian Caledonides and the sequential development history of the mountain belt, *in* Gee, D. G., and Sturt, B. A., eds., *The Caledonide orogen—Scandinavia and related areas*: Chichester, UK, Wiley, p. 919–930.
- Rubatto, D., and Hermann, J., 2001, Exhumation as fast as subduction?: *Geology*, v. 29, p. 3–6.
- Schumacher, R., 1991, Compositions and phase relations of calcic amphiboles in epidote- and clinopyroxene-bearing rocks of the amphibolite and lower granulite facies, central Massachusetts, USA: *Contributions to Mineralogy and Petrology*, v. 108, p. 196–211.
- Selbekk, R., and Skjerlie, K. P., 2002, Petrogenesis of the anorthosite dyke swarm of Tromsø, north Norway: Experimental evidence for hydrous anatexis of an alkaline mafic complex: *Journal of Petrology*, v. 43, p. 943–962.
- Selbekk, R. S., Skjerlie, K. P., and Pedersen, R. B., 2000, Generation of anorthositic magma by  $\text{H}_2\text{O}$ -fluxed anatexis of silica-undersaturated gabbro: An example from the north Norwegian Caledonides: *Geological Magazine*, v. 137, p. 609–621.
- Smith, D. C., 1984, Coesite in clinopyroxene in the Caledonides and its implications for geodynamics: *Nature*, v. 310, p. 641–644.
- Smyth, J. R., 1980, Cation vacancies and the crystal chemistry of breakdown reactions in kimberlitic omphacites: *American Mineralogist*, v. 65, p. 1185–1191.
- Steltenpohl, M., Hames, W., Andresen, A., and Markl, G., 2003, New Caledonian eclogite province in Norway and potential Laurentian (Taconic) and Baltic links: *Geology*, v. 31, p. 985–988.
- Stephens, M. B., and Gee, D. G., 1985, A tectonic model for the evolution of the eugeoclinal terranes in the central Scandinavian Caledonides, *in* Gee, D. G., and Sturt, B. A., eds., *The Caledonide orogen—Scandinavia and related areas*: Chichester, UK, Wiley, p. 953–970.
- Stephens, M. B., and Gee, D. G., 1989, Terranes and polyphase accretionary history in the Scandinavian Caledonides: *Geological Society of America, Special Paper*, v. 230, p. 17–30.
- Stevenson, J. A. 2005, High pressure partial melting of eclogite and garnet amphibolite rocks during decompression and heating, Tromsø Nappe, Norway: EOS (Transactions of the American Geophysical Union), v. 85 (47), Abstract T23C-03.

Yoshinobu, A. S., Barnes, C. G., Nordgulen, Ø., Prestvik, T., Fanning, M., and Pedersen, R. B., 2002, Ordovician magmatism, deformation, and exhumation in the

Caledonides of central Norway: An orphan of the Taconic orogeny?: *Geology*, v. 30, p. 883–886.

## Appendix

The reaction



has a gentle slope in the P-T space and has been used extensively as a reliable geobarometer (e.g., Ghent and Stout, 1981). We have used THERMOCALC (Powell and Holland, 1988) and the thermodynamic database of Holland and Powell (1998) to retrieve a linearized geobarometric expression for this reaction, given as

$$P(\text{GPa}) = 0.1171 + 0.001607T + 0.0001185T \ln K,$$

where K is the equilibrium constant expressed as

$$K = \frac{a_{py}^{Grt} * a_{grs}^{Grt} * a_{mu}^{Phe}}{a_{phl}^{Bt} * a_{an}^{Pl}}.$$

For biotite and muscovite we employed the

$$\text{activity models } a_{phl}^{Bt} = (X_{MgM2}^{Bt})^2 * X_{MgM1}^{Bt}, \text{ and}$$

$$a_{mu}^{Phe} = 4 * X_K^{Phe} * \frac{Al_{VI}^{Phe} - 2}{2} * X_{AlT1}^{Phe} * X_{SiT1}^{Phe},$$

respectively. The activity model for anorthite is from Holland and Powell (1992), and for garnet we used the formulations of Ganguly et al. (1996).